

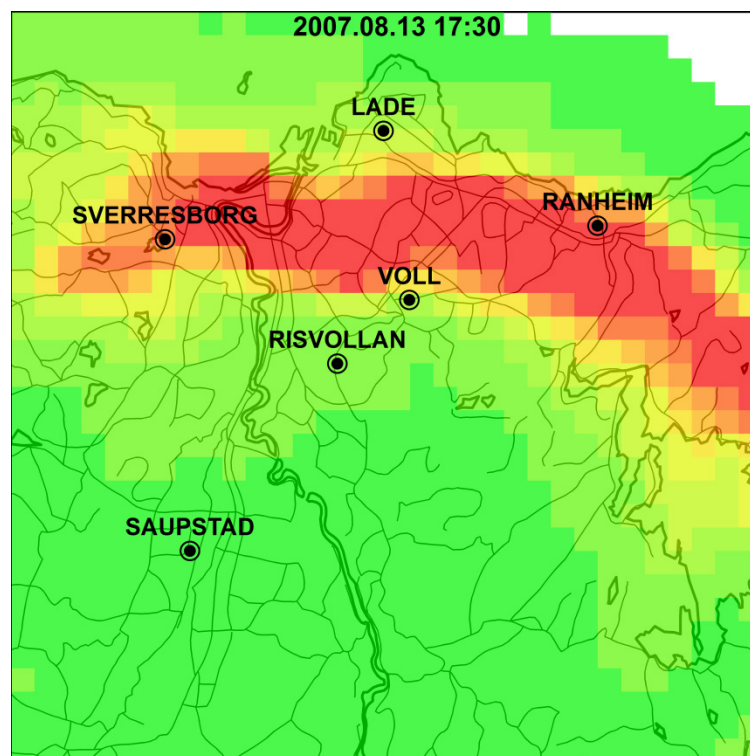
# Report

## Application of radar data to estimate distributed return periods of extreme rainfall events over Trondheim

Development of a tool for estimating return periods using radar data

**Author**

Yisak Sultan Abdella



# Report

## Application of radar data to estimate distributed return periods of extreme rainfall events over Trondheim

**KEYWORDS:**

Keywords

**VERSION**

1

**DATE**

2013-01-03

**AUTHOR(S)**

Yisak Sultan Abdella

**CLIENT(S)**

Trondheim Kommune

**CLIENT'S REF.**

Olav Nilssen

**PROJECT NO.**

12X832

**NUMBER OF PAGES:**

25

**ABSTRACT****Development of a tool for estimating return periods using radar data**

The return period of a given rainfall intensity is an important parameter for the Trondheim municipality since the drainage systems in Trondheim have been and are still being designed on the basis of a selected return period. Since rainfall is a spatially distributed phenomenon, a single event passing over a city can yield different return periods at different locations in the same city. In order to account for this spatial variability, a tool has been developed in this project for determining distributed return periods for rainfall events over Trondheim using the measurements from Rissa radar. The tool includes a method for adjusting radar rainfall using rain gauge measurements and an accumulation technique which accounts for storm movement and temporal variation in intensity. The tool has been tested on two extreme events which occurred on July 29 2007 and August 13 2007. The application on the two events has demonstrated a fully-automated estimation of distributed return periods using readily available data. For the particular rain gauge network in Trondheim, it has also been shown how areas of maximum intensity observed by the radar can be missed by all the gauges.

**PREPARED BY***for* Yisak Sultan Abdella**SIGNATURE****CHECKED BY**

Sjur Kolberg

**SIGNATURE****APPROVED BY**

Magnus Korpås

**SIGNATURE****REPORT NO.**

TR A7284

**ISBN**

978-82-594-3549-1

**CLASSIFICATION**

Unrestricted

**CLASSIFICATION THIS PAGE**

Unrestricted

# Document history

---

VERSION	DATE	VERSION DESCRIPTION
1	2013-01-03	Final version

## Sammendrag

To ekstreme nedbørshendelser i Trondheim den 29.juli og 13.august 2007 førte til overbelastning av avløpsnett og oversvømmelser med store skader (Risholt, 2009; Thorolfsson et al., 2008). Etter slike hendelser trenger Trondheim kommune en beregning av gjentaksintervallet for nedbøren for å avgjøre om den kan kalles en naturkatastrofe. En enkel nedbørshendelse som passerer over byen kan gi forskjellige gjentaksintervall for forskjellige steder i byen. For å kunne ta hensyn til denne romlige variasjonen beregnet Risholt (2009) et kart av maksimum nedbørsintensitet for de to ekstreme hendelsene ved å interpolere verdier fra seks punktmålinger av nedbør.

Selv et relativt tett nettverk av punktmålinger vil ikke klare å fange opp den store romlige variasjonen i nedbørsintensitet ved ekstreme nedbørsmengder. Nedbørsradaren på Rissa har siden 2006 samlet inn data over Trondheim. Den har en oppløsning på ca 500 m og gir øyeblikksbilder hvert 5 og 10. minutt. Radardataene kan sammen med punktmålinger gi et mer realistisk bilde av hvordan en ekstrem nedbørshendelse fordelere seg over Trondheim. Målet med dette studiet er derfor å utvikle et verktøy som kan beregne kart for gjentaksintervall for ekstreme nedbørshendelser over Trondheim ved å bruke radardata fra Rissa sammen med data fra seks nedbørsmålere.

Verktøyet som ble utviklet tar i bruk rådata fra værradaren på Rissa og har følgende innhold.

- **Korreksjon av signaldemping.** Radarsignalet dempes av nedbør, og spesielt ved høye intensiteter er denne korreksjonen viktig for å få bedre estimat av nedbørsintensiteten i områder som ligger bak en kraftig nedbørscelle.
- **Projeksjon til kartesianske koordinater.** Radardata kommer i polarkoordinater, og de projiseres til et regulært rutenett på 500x500 m.
- **Z-R konvertering.** Radaren måler reflektivitet ( $Z$ ) som transformeres til nedbørsintensitet ( $R$ ) ved hjelp av en ikke-lineær ligning.
- **Interpolering i tid ved å bruke adveksjon.** Radaren gir øyeblikksbilder hvert 5. og 10. minutt. Det beregnes øyeblikksbilder med 1 minutts oppløsning ved å ta hensyn til hvordan nedbøren forflytter seg mellom to påfølgende bilder (adveksjon) og hvordan nedbørsintensiteten varierer mellom to påfølgende bilder.
- **Justering ved å bruke punktmålinger.** Nedbørsintensiteter beregnet fra radaren justeres slik at det oppnås samme akkumulerte nedbørsmengder som observert ved nedbørsstasjonene.
- **Akkumulering i tid.** Basert på kart med 1-minutts nedbør, kan nå akkumulert nedbør beregnes for ulike varighet.
- **Beregning av gjentaksintervall.** Basert på intensitet-varighet-frekvens (IVF) kurve fra Voll, relateres akkumulerte nedbørsmengder for ulike varigheter til gjentaksintervall for ulike varigheter. Gjentaksintervallet kan beregnes for en spesifisert varighet, for den varigheten som gir størst gjentaksintervall for en majoritet av pikslene, eller for den varigheten som gir størst gjentaksintervall i hver piksel.

Verktøyet ble brukt for å beregne gjentaksintervallet for de to ekstreme nedbørshendelsene over Trondheim i 2007 og følgende konklusjoner kan gis.

- Verktøyet gir en full-automatisk beregning av gjentaksintervall, men krever tilrettelegging av data
- Den adveksjons-baserte interpoleringen hjelper til å fange opp tids-variasjonen i nedbørsintensitet og er essensiell for å oppnå bedre beregninger av akkumulerte nedbørsmengder.
- Etter justering basert på bakkemålinger kan radardata fra Rissa brukes for å beregne kart av gjentaksintervall for nedbør med 500 meters oppløsning.
- Akkumulerte nedbørskart basert på radarmålinger gir romlig fordeling som er veldig forskjellig fra kartene basert kun på å interpolere verdier fra nedbørsmålere. Dette skyldes at de interpolerte kartene har mindre informasjon om den romlige fordelingen av nedbør.
- Nettet med 6 nedbørsmålere over Trondheim kan gå glipp av områder med maksimal nedbørsintensitet når en ekstrem konvektiv nedbørshendelse passerer over byen.

# Table of contents

<b>Sammendrag .....</b>	<b>3</b>
<b>1 Introduction .....</b>	<b>5</b>
<b>2 Study area and data.....</b>	<b>6</b>
<b>3 Methodology.....</b>	<b>7</b>
3.1 Attenuation correction .....	7
3.2 Polar to Cartesian grid conversion.....	8
3.3 Z-R conversion.....	8
3.4 Advection .....	8
3.5 Adjustment using rain gauge measurements .....	9
3.6 Return period estimation.....	10
<b>4 Case studies .....</b>	<b>11</b>
4.1 Event 1: July 29 2007 .....	11
4.2 Event 2: August 13 2007 .....	16
<b>5 Summary and conclusions.....</b>	<b>22</b>
<b>6 Further research.....</b>	<b>23</b>
<b>7 References .....</b>	<b>24</b>

## 1 Introduction

Two extreme rainfall events over the city of Trondheim on August 13 2007 and July 29 2007 caused overloading of the urban drainage system. The flooding from these events resulted in large damages (Risholt, 2009; Thorolfsson et al., 2008). After such flooding incidents the Trondheim municipality, which is the operator of the public drainage system, needs an assessment of the return period of the associated rainfall events in order to produce a statement of liability or of natural disaster. The return period of a given rainfall intensity is an important parameter since the drainage systems in Trondheim have been and are still being designed on the basis of a selected return period.

Since rainfall is a spatially distributed phenomenon a single event passing over a city can yield different return periods at different locations in the same city. In order to account for this spatial variability, analysis of extreme rainfall events over urban areas and estimation of their return periods have usually been based on point measurements from a network of rain gauges. Risholt (2009) estimated maps of maximum intensities for the two extreme events over Trondheim by interpolating values from six gauges within the city. However, rainfall can have very inhomogeneous spatial pattern making it difficult to get a representative description of an event even when a dense network of gauges is present. This is particularly true in case of convective rainfall which is often characterized by high spatial variability and fast temporal evolution. Most of the rainfall events causing damage in urban areas, including the two events in Trondheim, have significant convective elements. Therefore, measurements from gauges should be complemented with additional sources of information in order to obtain better estimates of spatially distributed return periods.

One such source which provides spatially distributed measurement is weather radar. Rainfall over Trondheim has been sampled since 2006 with a C-band Doppler radar located in Rissa and operated by the Norwegian Meteorological Institute (met.no). One of the main challenges in using radar data quantitatively is the uncertainty involved in converting a measurement of reflectivity ( $Z$ ) made aloft to the corresponding surface rainfall rate ( $R$ ). The error due to this uncertainty is usually reduced by adjusting radar rainfall using measurements from gauges on the ground. The other challenge particularly relevant for urban hydrology is effect of sampling interval on rainfall accumulations. The measurements from this radar are available as instantaneous maps with alternating time intervals of 5 and 10 minutes. As the determination of return period requires the mean intensities over several durations, these maps have to be accumulated over the corresponding durations. Significant error can be introduced if this accumulation process is carried out as a simple addition of maps under the assumption that the precipitation field remains stationary in space and intensity during the sampling interval (Fabry et al., 1994; Hannesen and Gysi, 2002; Piccolo and Chirico, 2005). The magnitude of this error is relatively higher for fast moving and evolving storms.

The objective of this project is to develop a tool for determining distributed return periods for rainfall events over Trondheim using the measurements from Rissa radar. In order to address the challenges mentioned above the tool includes a method for adjusting radar rainfall using rain gauge measurements and an accumulation technique which accounts for storm movement and temporal variation in intensity. The tool has been tested on the two extreme events in the summer of 2007.

The report is organized as follows. Section 2 gives an overview of the study area and the available data. The various components of the tool are described in section 3. Results from the application of the tool on the two events are presented in section 4. In section 5, a summary is given and some conclusions are drawn based on the application on the events. Finally some issues for further research are identified and listed under section 6.

## 2 Study area and data

The analysis has been carried out for a 16x16 km rectangular domain centred on Trondheim (Figure 1). Radar reflectivity data from the Rissa Radar were obtained from met.no for use in this project. The radar is located in Olsøyheia in the municipality of Rissa and is situated at an elevation of 616m above sea level. It is a C-band Doppler radar with a half-power beam width of 1 degree. The radar has two scan sequences: one with 12 elevation angle scanning and a second with 10. Both sequences are repeated at a frequency of 15min with the second strategy executed 5min after the first one. This gives an effective temporal resolution of 5 and 10 min. The raw radar data obtained consist of volume scans of radar reflectivity collected in polar coordinates in the form of plan position indicators (PPIs). Stationary echoes in the lowest PPIs are removed during data acquisition by using a Doppler filter. Unfortunately, the events analysed here occurred within the period during which Doppler filtering was not activated while executing the second scan sequence. Review of the lowest PPI from this scan revealed too much contamination by ground clutter. Therefore, only data from the lowest PPI of the first sequence has been used in this project. The exclusion of the second scan reduced the temporal resolution of the radar data to 15min. The azimuthal and radial resolutions of the lowest PPI used are 1degree and 250m respectively.

Rainfall measurements on the ground were available from six tipping-bucket rain gauges situated in Trondheim (Figure 1). All the gauges have a bucket capacity of 0.1mm and measure accumulated rainfall by recording the number of bucket tips every minute. Data from four of these gauges (Lade, Ranheim, Saupstad, Sverresborg) were obtained from Trondheim municipality while data from Risvollan and Voll were obtained from the Norwegian Water Resources and Energy Directorate (NVE) and met.no respectively.

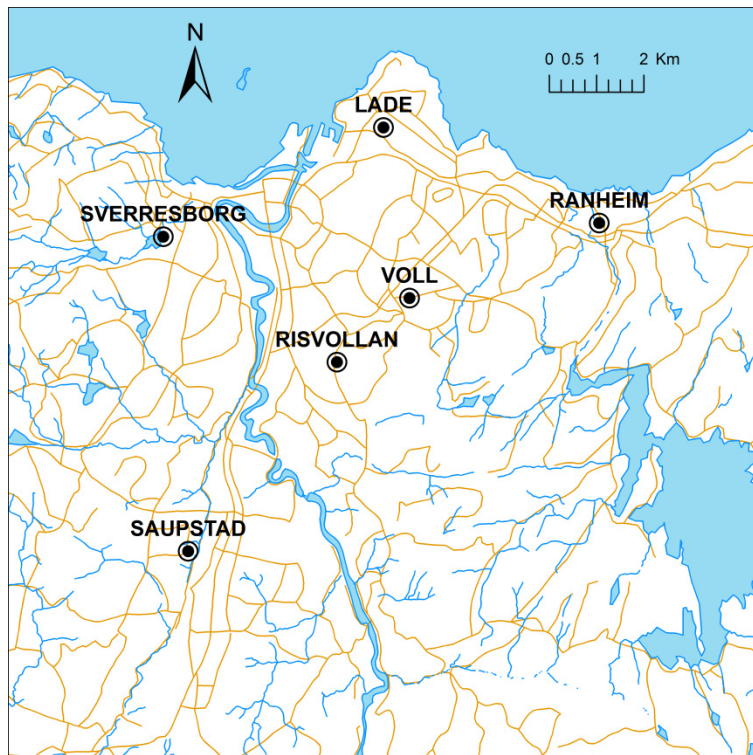


**Figure 1.** Study area and location of rain gauges. The study area has a dimension of 16x16km.

### 3 Methodology

The estimation of distributed return period from radar data involves a number of processing steps. Each of these steps has been implemented as a component in the tool developed within the project. The tool enables the automated generation of return period maps for selectable durations and the duration for which the return period is the longest for majority of the pixels in the map. The main inputs required are radar reflectivity maps, rain gauge measurements and an Intensity-Duration-Frequency (IDF) curve. Figure 2 presents the processing steps and the inputs as a flow chart. Description of the different steps is given in sections 3.1-3.6.

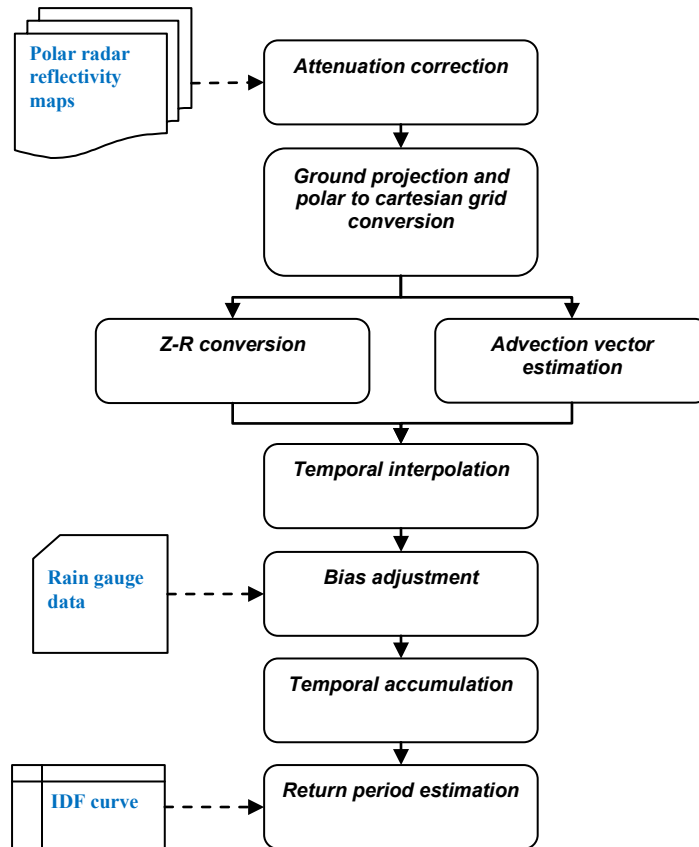


**Figure 2.** Processing steps included in the tool. The blue text indicates input data.

#### 3.1 Attenuation correction

Rain-induced signal attenuation can become a significant source of error for C-band radars, particularly during heavy rainfall (Delrieu et al., 1999,2000; Uijlenhoet and Berne, 2008). And since the tool is mainly targeted towards extreme events, the correction of error due to attenuation is relevant here. This correction is the first step in the tool and it uses reflectivity maps in polar coordinate. It is carried out separately for each ray by applying the following equation at each range,  $r$  (Delrieu et al., 1999; Hazenberg et al., 2011)

$$Z(r) = \frac{Z_m(r)}{\left[1 - \frac{2\ln 10}{10^d} \int_0^r \left(\frac{Z_m(s)}{c}\right)^{1/d} ds\right]^d} \quad (1)$$

$Z(r)$  and  $Z_m(r)$  are the true and measured radar reflectivity respectively.  $c$  and  $d$  are parameters of the power-law relationship between reflectivity and specific attenuation.

### 3.2 Polar to Cartesian grid conversion

In this processing step the polar reflectivity maps corrected for attenuation are projected to the ground level assuming standard atmospheric refraction of the radar beam (Doviak and Zrníć, 1993). Then the projected polar maps are converted to cartesian maps through area-weighted interpolation. For each cartesian pixel, these weights are the overlapping areas between the cartesian pixel and all polar pixels which intersect with the cartesian pixel.

### 3.3 Z-R conversion

The cartesian reflectivity maps are converted to equivalent rainfall rate maps by using a power law relationship:

$$Z = aR^b, \quad (2)$$

where the parameters  $a$  and  $b$  are a function of the raindrop size distribution and vary with precipitation type. The Marshall-Palmer Z-R relation with parameters  $a = 200$  and  $b = 1.6$  (Marshall and Palmer, 1948) is used as the default conversion.

### 3.4 Advection

The instantaneous rainfall rate maps obtained after the Z-R conversion still have a temporal resolution of 15min, as the raw input data. Since the remaining steps in the tool require accumulated rainfall maps, an algorithm has been implemented to first generate maps in between the 15min interval before performing accumulation. The positive effect of such temporal interpolation on the quality of accumulated values has been documented in previous studies (Fabry et al., 1995; Liu and Krajweski, 1996; Hannesen and Gysi, 2002). Temporal interpolation has been incorporated in the tool as a two-step procedure: estimation of the advection vector and generation of maps at user-specified subintervals.

The advection vector estimation is based on a well known maximum cross-correlation technique (Li et al., 1995). The technique starts by taking the first map from two subsequent maps and extracting a rectangular domain for which advection velocity and direction is to be determined. Then the two dimensional array constituting this domain is horizontally shifted in all directions within a given radius and compared with the corresponding array from the consecutive map. The comparison is made by computing the correlation coefficient between each array-pair. Finally the location of the array in the second map for which the correlation is maximum is selected as the endpoint of the translation vector. The search radius is defined by the user and it reflects the displacement resulting from the expected maximum velocity.

With the advection vector estimated as displacements in the x ( $disp_x$ ) and y ( $disp_y$ ) direction, the interpolation of rainfall maps is carried out assuming a linear variation in intensity (Fabry et al., 1995; Liu and Krajweski, 1996). Suppose  $R(x, y, t_0)$  and  $R(x, y, t_1)$  are two subsequent rainfall intensity maps at time  $t_0$  and  $t_1$  respectively, with time interval  $\Delta t = t_1 - t_0$ . Then the intensity for each pixel  $i$  in map  $R(x, y, t)$  at time  $t$ , where  $t_0 \leq t \leq t_1$ , can be approximated as

$$R(x_i, y_i, t) \approx w_0 R(x_i - w_0 disp_x, y_i - w_0 disp_y, t_0) + w_1 R(x_i + w_1 disp_x, y_i + w_1 disp_y, t_1), \quad (3)$$

in which the weighting factors  $w_0$  and  $w_1$  are defined as

$$w_0 = \frac{t - t_0}{\Delta t} \quad (4)$$

$$w_1 = \frac{t_1 - t}{\Delta t} \tag{5}$$

The above procedure has been illustrated in Figure 3.

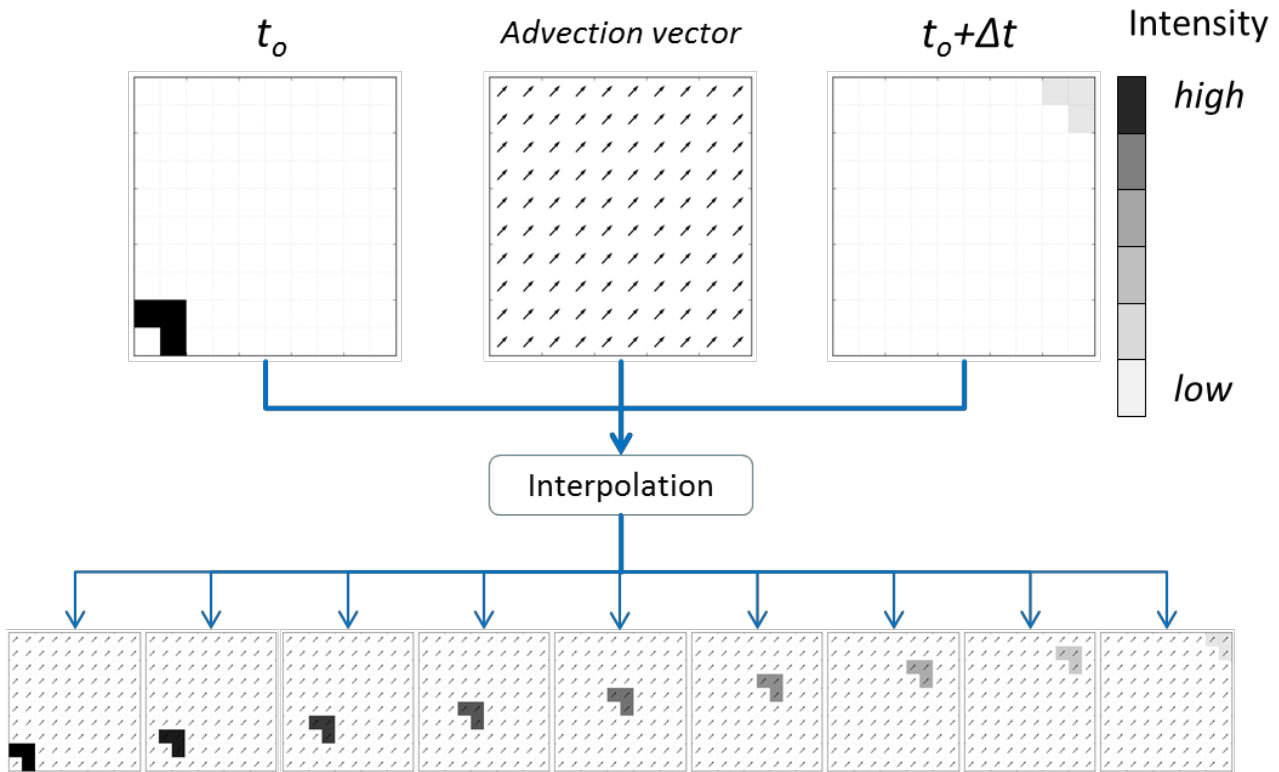


**Figure 3.** Temporal interpolation using global advection vector and assuming linear variation in intensity.

### 3.5 Adjustment using rain gauge measurements

Rainfall estimates from radar measurements are subject to a number of errors (for a recent review, see Villarini and Krajewski, 2010). The error sources most relevant to the data in this project are those associated to uncertainties in the parameters of the Z-R conversion and the attenuation correction. Non-uniformity of the vertical profile of reflectivity (VPR) is also a dominant source of error in the study region (Abdella and Alfredsen, 2010). In this project, however, the use of data from a low elevation scan close to the radar and the fact that the events of interest are summer-time convective events significantly reduce the influence of VPR.

Because of the above factors, information derived from radar measurements is often combined with or adjusted by rain gauge observations to obtain more accurate precipitation estimates (Abdella and Alfredsen, 2010; Steiner et al., 1999). A similar procedure has been implemented in the tool as a mean-field bias (MFB) adjustment (Steiner et al., 1999). Using  $n$  number of gauges the MFB is computed for each time-step of the interpolated map-series as

$$MFB = \frac{\sum_{i=1}^n G_i}{\sum_{i=1}^n R_i} \tag{6}$$

where  $G_i$  and  $R_i$  are gauge and radar precipitation accumulations respectively at gauge location  $i$ . Radar precipitation corresponding to each gauge location is extracted as the value of the single radar pixel over the gauge or the average value of the nine radar pixels centered at the gauge. The MFB computation is done on accumulated values in order to reduce the noise in the data at finer time resolution. The time window for the accumulation is centered on the time-step at which the MFB is to be applied and the length of this window (accumulation duration) is selected by the user. The adjustment is carried out by applying the MFB as a spatially constant but temporally variable scaling factor.

### 3.6 Return period estimation

The final processing step in the tool is the estimation of the return periods for all the pixels covering the study area. The inputs for this step are the time-series of adjusted radar precipitation maps and an IDF curve. The return period can be estimated for any user-selected duration. But most importantly, the duration for which the return period is longest for the majority of the pixels is identified and the return period corresponding to this duration is estimated from the IDF curve. Maps of maximum intensities for a selected duration are also given as outputs. It is important to note that, for the same event, the duration which gives the longest return period at one pixel may not be the same duration which gives the longest return period at another pixel. Moreover, in a map of return periods for the same duration, the time windows from which the intensities are computed may not be the same for the pixels of the same map. For example, suppose that the duration which gives the longest return period for an event at pixel  $a(x_a, y_a)$  is 5min and that the corresponding maximum intensity occurs within the time window 15:00 – 15:05. Then for the same event at another pixel  $b(x_b, y_b)$  in the same area, it is fully possible that (1) the duration with the longest return period is still 5min but resulting from the maximum intensity occurring within 15:07-15:12 or (2) the duration with the longest return period is 10min and resulting from the maximum intensity occurring within 15:01-15:11. These are two of many other possibilities.

## 4 Case studies

The tool developed was tested on two extreme rainfall events in Trondheim which occurred on July 29 and August 13 2007. The following steps were executed for both events:

- the polar radar reflectivity maps at 15min sampling interval were corrected for attenuation using the parameters  $c = 7.34 \times 10^5$  and  $d = 1.344$  in Eq. 1.
- the corrected polar maps were projected to the ground level and converted to cartesian maps with a spatial resolution of 500x500m
- the cartesian reflectivity maps were converted to maps of rainfall rates using the parameters  $a = 200$  and  $b = 1.6$  in the Z-R relation (Eq. 2)
- the advection direction and velocity were calculated by maximizing the correlation between two consecutive cartesian reflectivity maps in logarithmic scale, i.e.  $10 \cdot \log(Z)$
- using the resulting advection vector, the radar rainfall rate maps were interpolated in time at 1min intervals assuming a linear variation in rainfall rate
- time-series of MFBs were calculated for each interpolated map for an accumulation duration of 11min using all the six gauges in Trondheim
- adjusted rainfall rate maps were generated by multiplying each interpolated map by the corresponding MFB
- maps of return periods were estimated for various durations using the IDF curve generated for Voll station
- the longest return period for each individual pixel was identified together with the corresponding duration
- the duration which results in the longest return period for the majority of the pixels was identified

The results from the two events are given in sections 4.1 and 4.2.

### 4.1 Event 1: July 29 2007

8 hours of data from 23:00 to 07:00 were processed for the event of July 29 2007. The temporal evolution of the rainfall intensity at the gauge locations for these 8 hours is given in Figure 4. The radar underestimates the intensity for most of the period at all gauge locations. The MFB adjustment has removed a significant portion of the underestimation. The temporal pattern of rainfall measured by the gauges has, to some extent, been captured by the corrected radar rainfall estimates. This matching of the temporal pattern indicates the positive impact of the advection-based temporal interpolation. As an example, the 1min rainfall intensity maps interpolated between the two maps sampled at 23:15 and 23:30 are shown in Figure 5.

The following durations were selected for the estimation of maximum intensity and return period: 5, 10, 15, 20, 30, 45, 60, 120, 240, 360 and 420 min. After this estimation, maps of longest return periods and the corresponding durations were generated and are given as Figure 9 and Figure 10 respectively. The durations which resulted in the longest return period for most of pixels were identified to be 30 and 360 min. However, considering how short the response times of urban catchments are, the 30 min duration is the most relevant with respect to urban flooding. In addition to this general consideration, it was also found that the longer return periods for the 360 min duration were due to higher rainfall accumulations from two high intensity episodes separated by 360 min. These two episodes can be easily observed in the plots of Figure 4. Following the above considerations, the 30 min duration was selected as the critical duration for the event of July 29 2007.

Maps of maximum rainfall intensity and return period for the 30 min duration are given in Figure 7 and Figure 8 respectively. The identification of maximum intensity first requires the generation of accumulated values for the various durations. An example of a map with accumulated values for the 30 min duration within the time window 23:15-23:45 is shown in Figure 6.

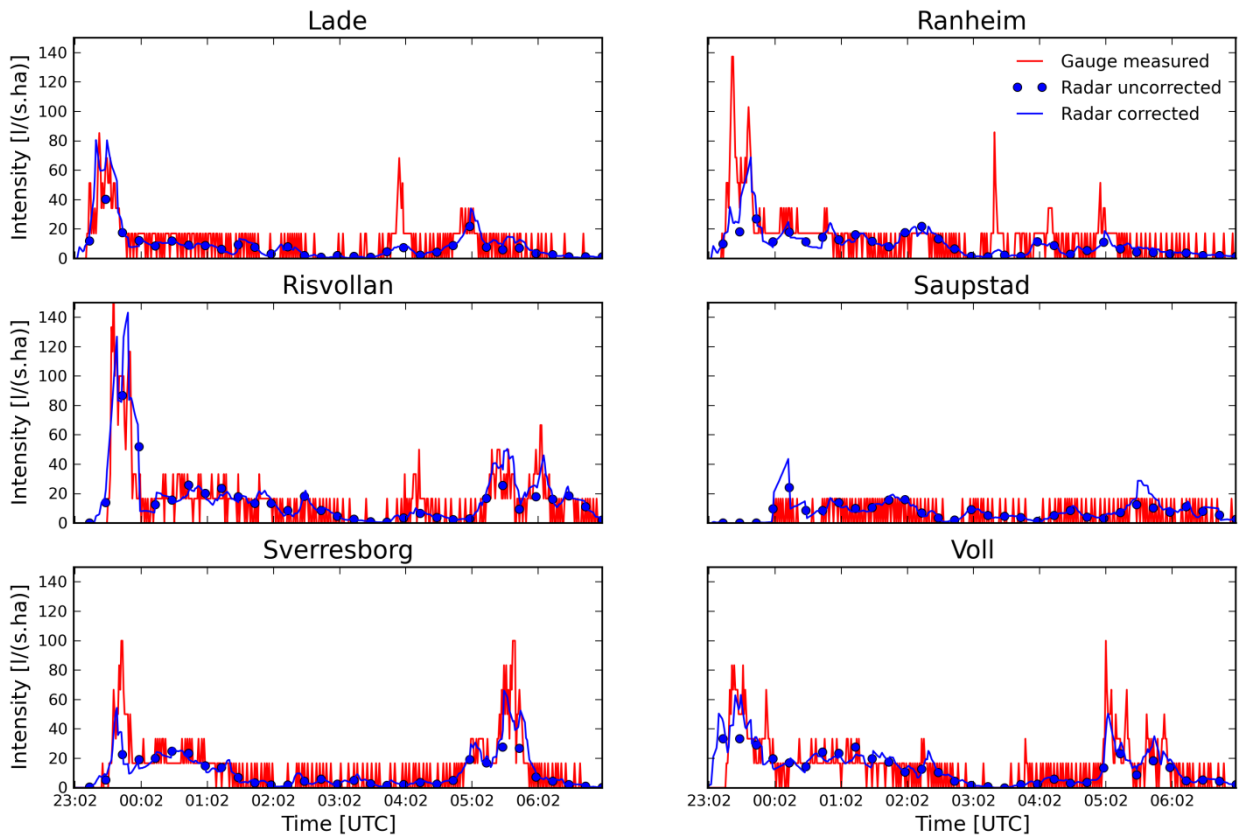


**Figure 4.** Comparisons of rainfall intensities from the six gauges and the corresponding radar pixels for the event on July 29 2007. The red line corresponds to the intensities measured by the gauge every 1min. The blue dots correspond to the pixel values extracted from the radar rainfall maps obtained after Z-R conversion of the 15-min radar reflectivity (Z) maps using the parameters  $a = 200$  and  $b = 1.6$ . The blue line corresponds to pixel values extracted from the 1-min radar rainfall rate (R) maps obtained after advection-based temporal interpolation and MFB adjustment.

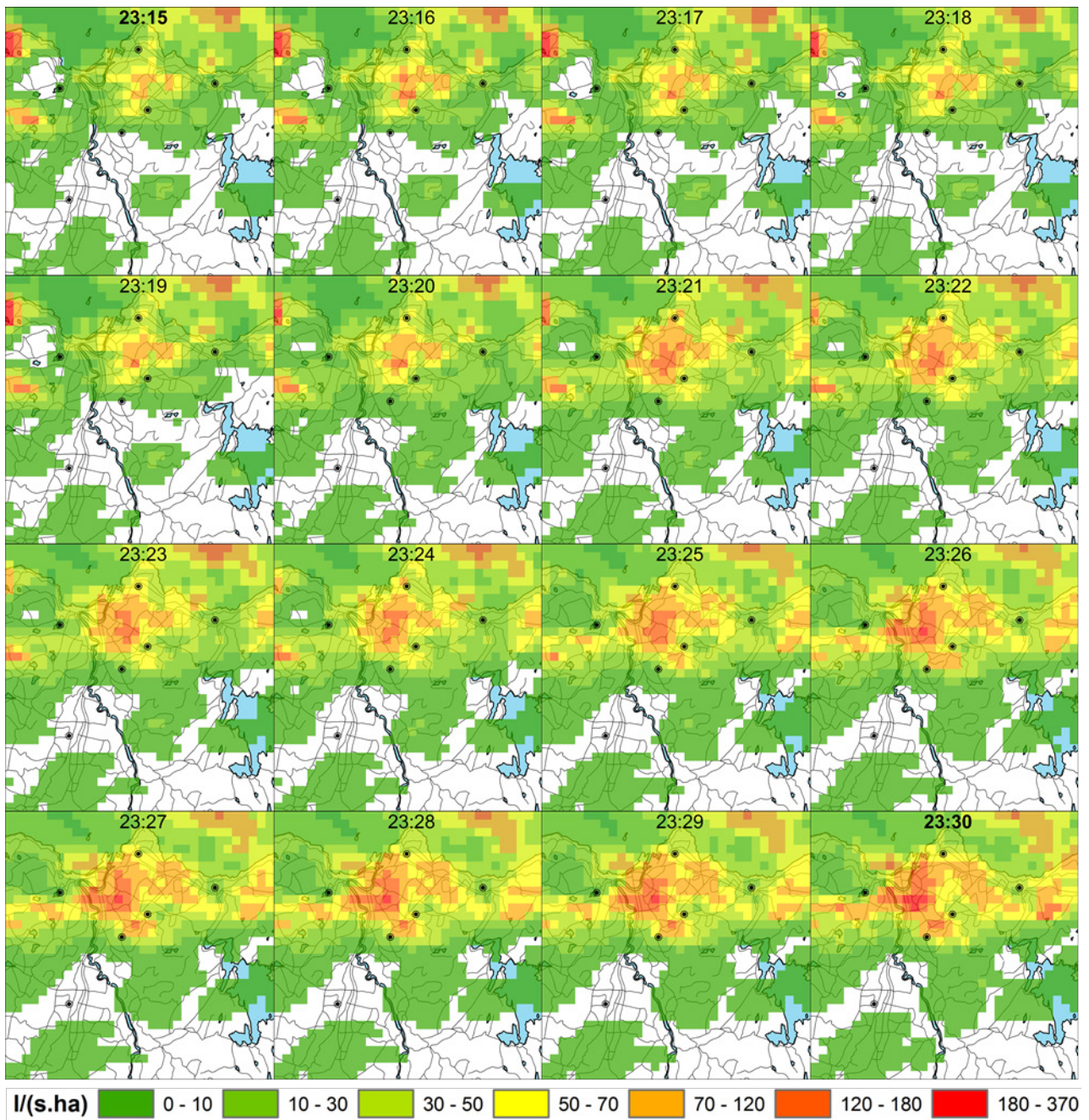


**Figure 5.** Maps of rainfall intensity interpolated between 23:15 and 23:30 for the event on July 29 2007. The maps at 23:15 and 23:30 were generated from measured values while the rest of the maps were generated from interpolation. The black circular dots represent the locations of the six gauges.

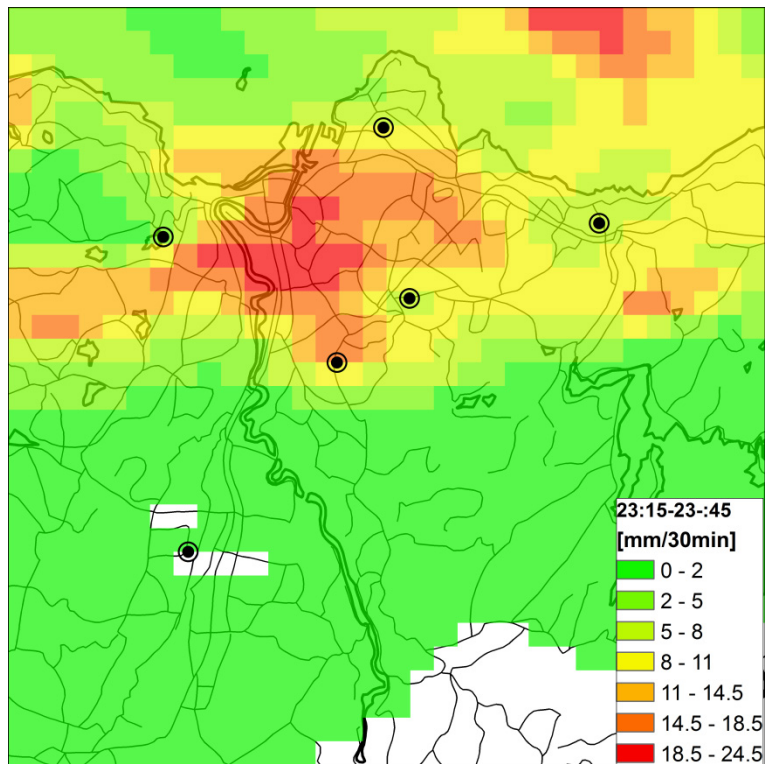


**Figure 6.** Rainfall accumulation for the period 23:15-23:45 for the event on July 29 2007.

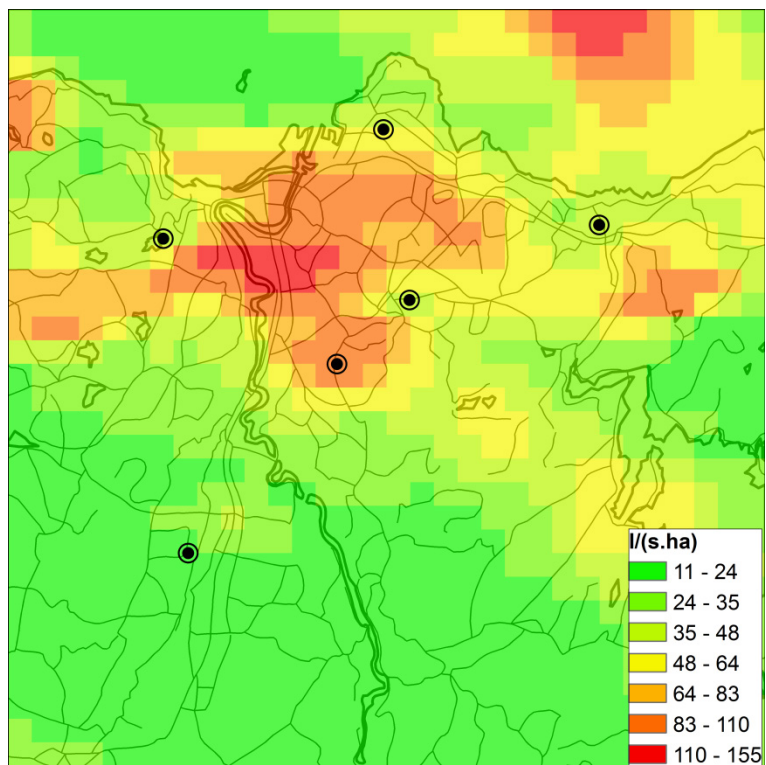


**Figure 7.** Maximum rainfall intensity for 30 min duration for the event on July 29 2007.

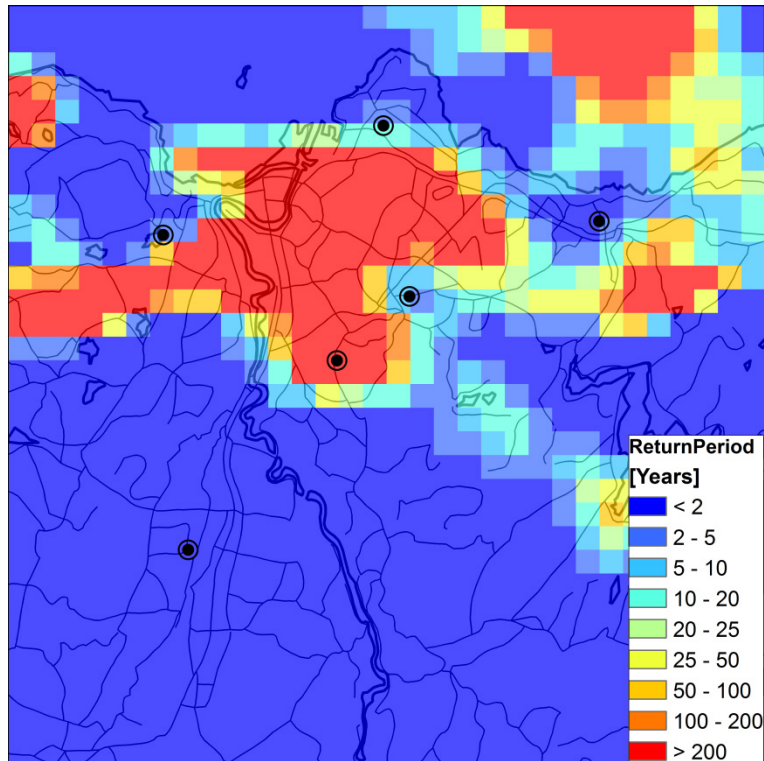


**Figure 8.** Return periods corresponding to the maximum intensities for 30 min duration for the event on July 29 2007. The return periods of all the pixels are estimated for the same duration, which is 30 min.

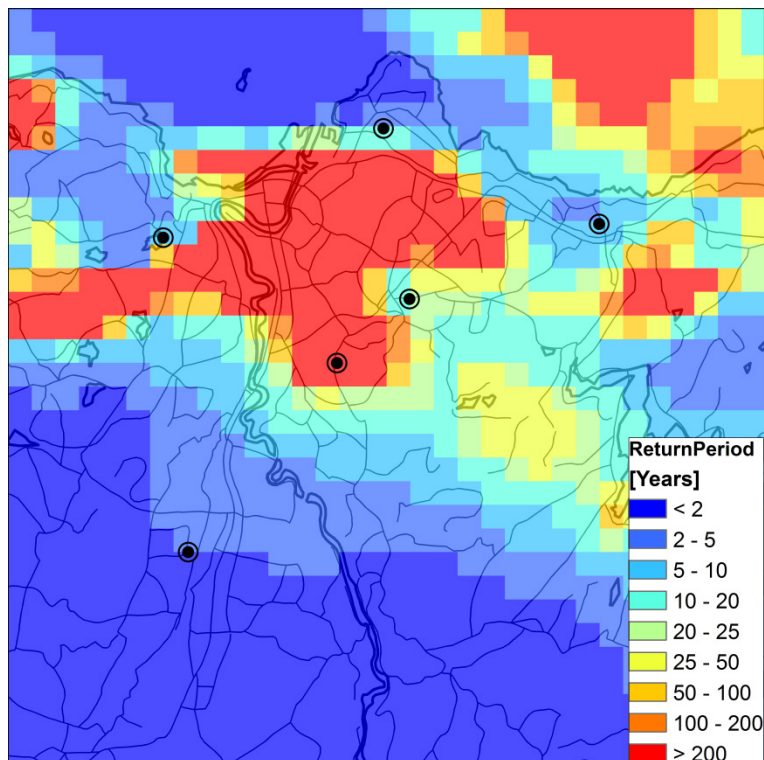


**Figure 9.** Longest return periods for the event on July 29 2007. The return period for each pixel corresponds to the longest period out of the return periods estimated for the maximum intensities for the following durations: 5, 10, 15, 20, 30, 45, 60, 120, 240, 360 and 420 min.

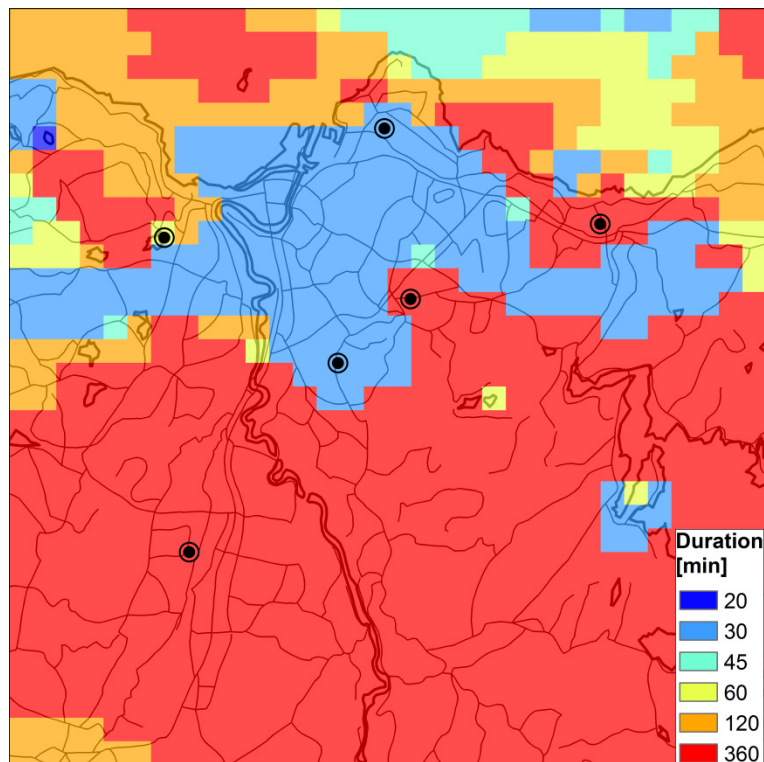


**Figure 10.** Durations corresponding to the longest return periods shown in the map of Figure 9.

## 4.2 Event 2: August 13 2007

1.5 hours of data from 17:00 to 18:30 were processed for the event of August 13 2007. The temporal evolution of the rainfall intensity at the gauge locations for these 1.5 hours is given in Figure 11. The radar underestimates the intensity for most of the period at all gauge locations except Ranheim. The MFB adjustment has removed a significant portion of the underestimation while it has resulted in overestimation at Ranheim. This overestimation at Ranheim shows one weakness of the MFB adjustment in that it cannot cope with errors which significantly vary in space. The temporal pattern of rainfall measured by the gauges has, to a large extent, been captured by the corrected radar rainfall estimates. This matching of the temporal pattern indicates the importance of the advection-based temporal interpolation. As an example, the 1min rainfall intensity maps interpolated between the two maps sampled at 17:15 and 17:30 are shown in Figure 12.

The following durations were selected for the estimation of maximum intensity and return period: 1, 5, 15, 15 and 20 min. After this estimation, maps of longest return periods and the corresponding durations were generated and are given as Figure 16 and Figure 17 respectively. The duration which resulted in the longest return period for most of pixels was identified to be 5 min. The 5 min duration was selected as the critical duration for the event of August 13 2007.

Maps of maximum rainfall intensity and return period for the 5 min duration are given in Figure 14 and Figure 15 respectively. The identification of maximum intensity first requires the generation of accumulated values for the various durations. An example of a map with accumulated values for the 5 min duration within the time window 17:25-17:30 is shown in Figure 13.

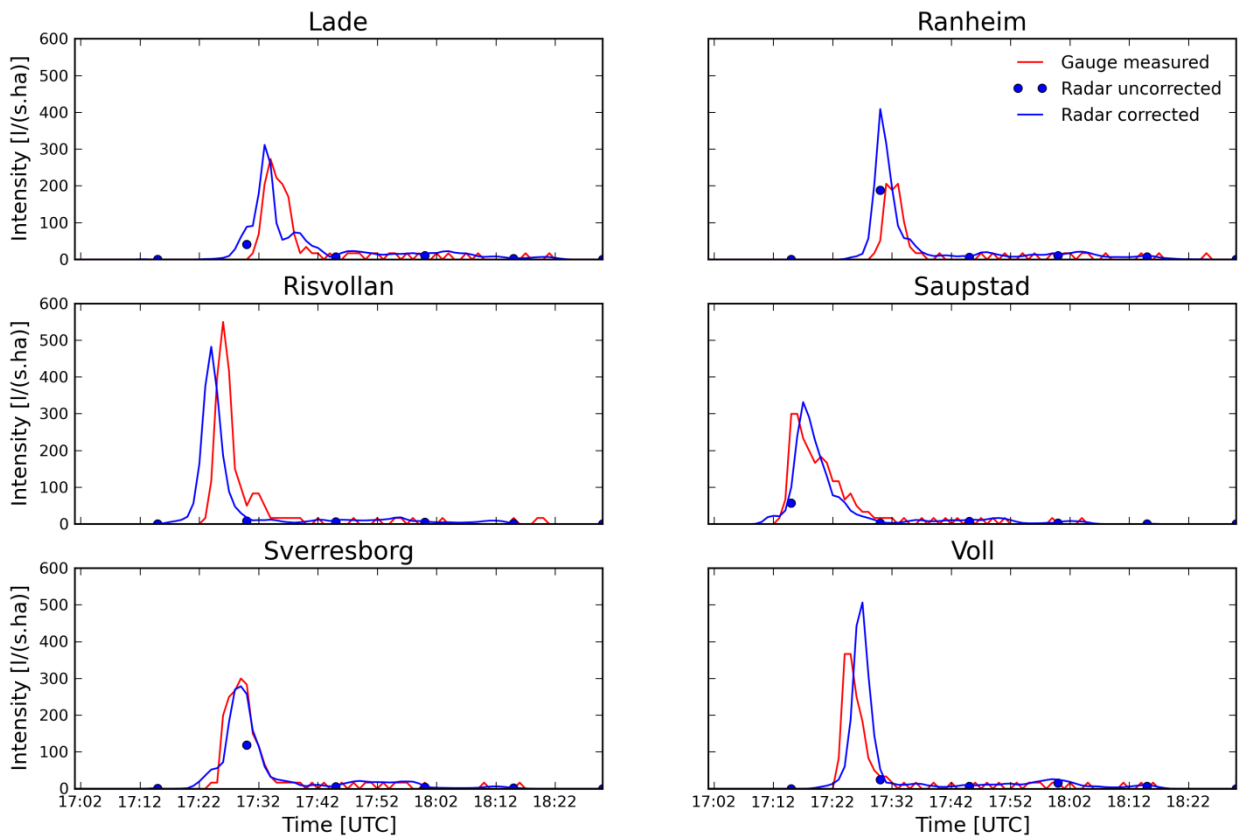


**Figure 11.** Comparisons of rainfall intensities from the six gauges and the corresponding radar pixels for the event on August 13 2007. The red line corresponds to the intensities measured by the gauge every 1min. The blue dots correspond to the pixel values extracted from the radar rainfall maps obtained after Z-R conversion of the 15-min radar reflectivity ( $Z$ ) maps using the parameters  $a = 200$  and  $b = 1.6$ . The blue line corresponds to pixel values extracted from the 1-min radar rainfall rate ( $R$ ) maps obtained after advection-based temporal interpolation and MFB adjustment.

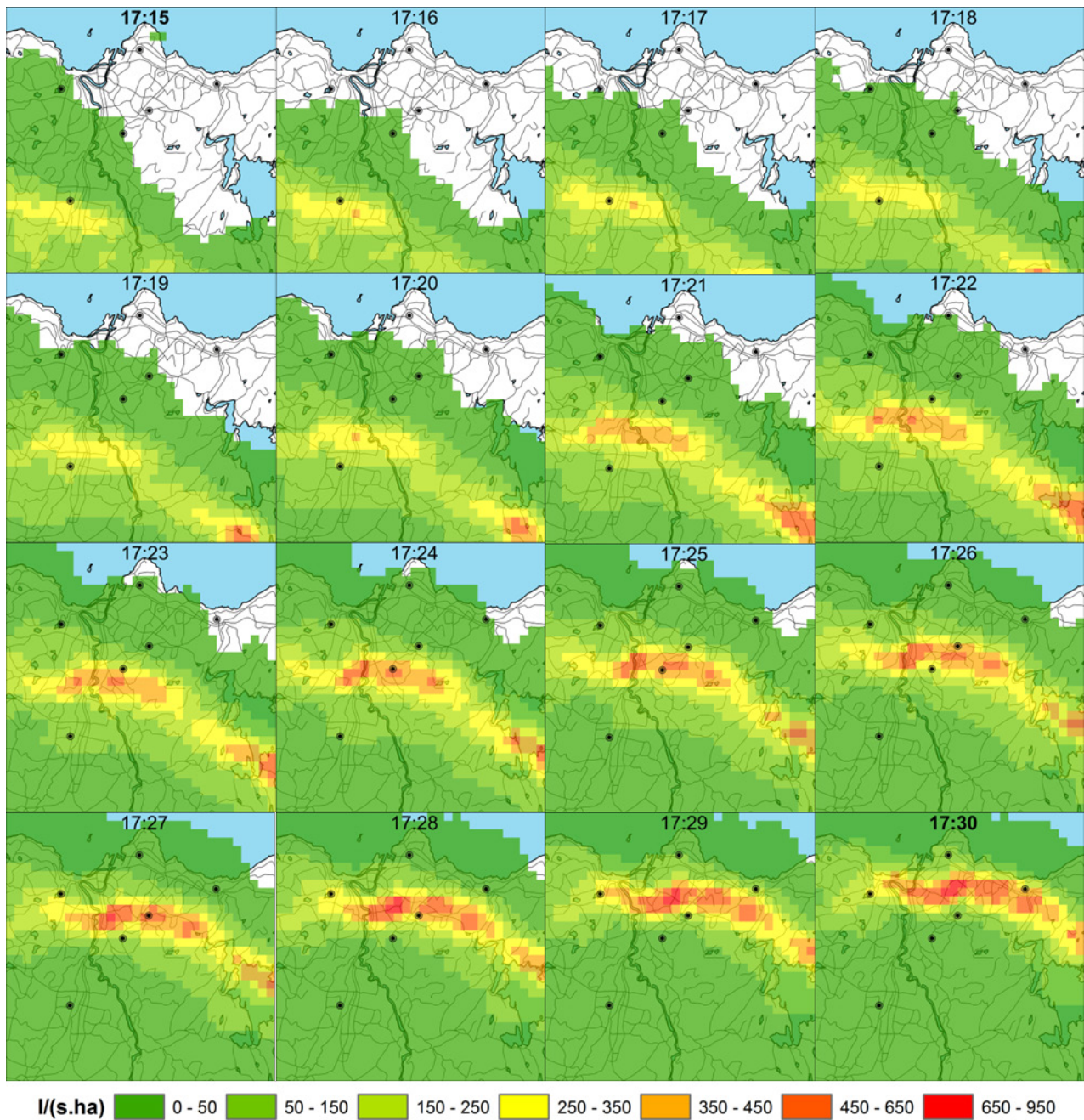


**Figure 12.** Maps of rainfall intensity interpolated between 17:15 and 17:30 for the event on August 13 2007. The maps at 17:15 and 17:30 were generated from measured values while the rest of the maps were generated from interpolation. The black circular dots represent the locations of the six gauges.

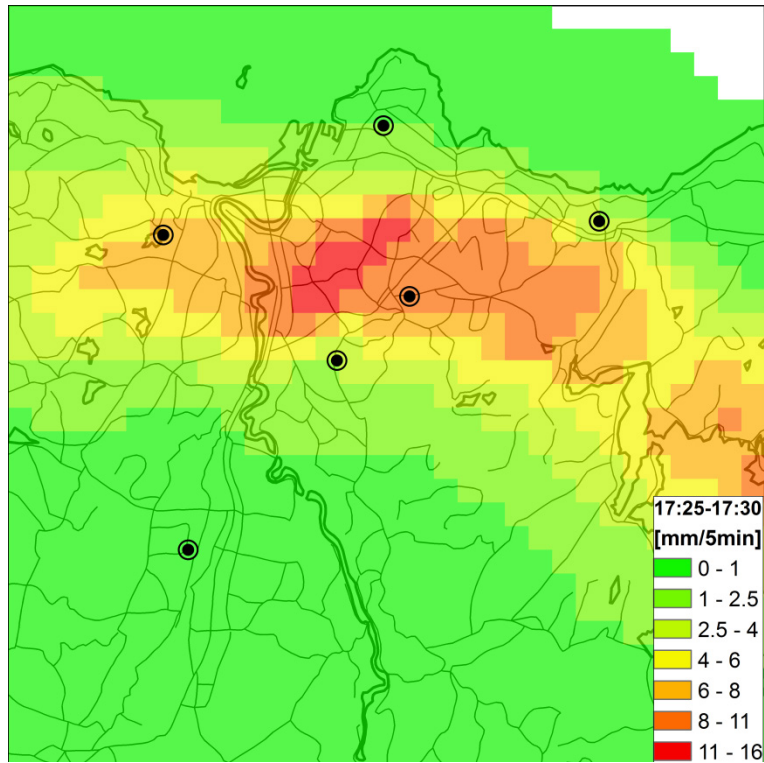


**Figure 13.** Rainfall accumulation for the period 17:25-17:30 for the event on August 13 2007.

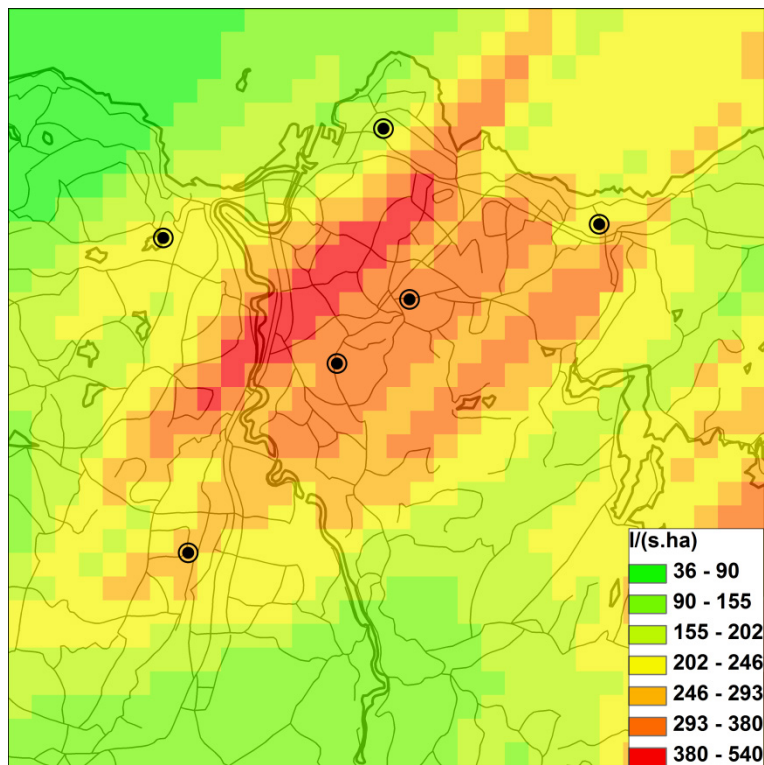


**Figure 14.** Maximum rainfall intensity for 5 min duration for the event on August 13 2007.

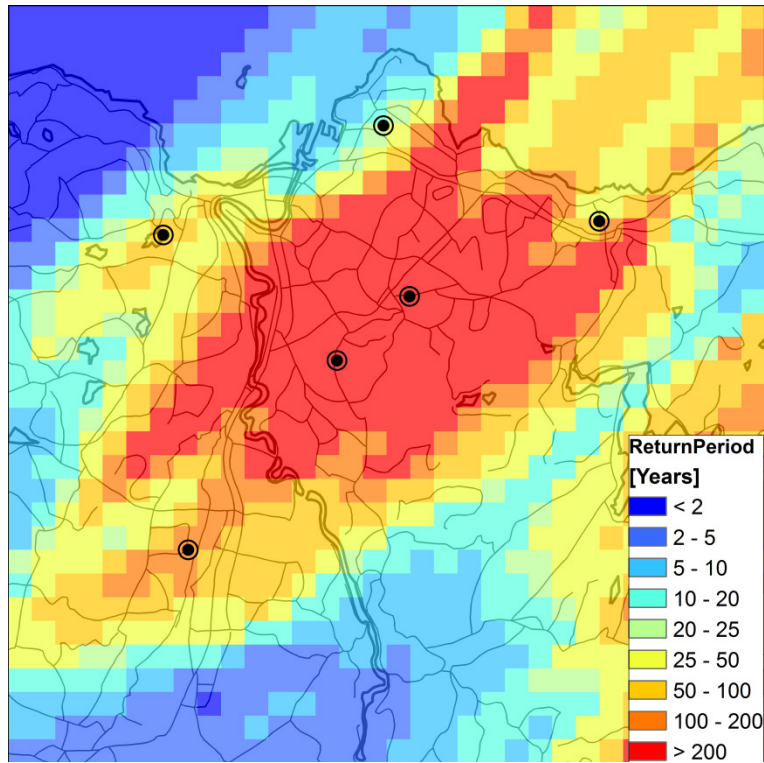


**Figure 15.** Return periods corresponding to the maximum intensities for 5 min duration for the event on August 13 2007. The return periods of all the pixels are estimated for the same duration, which is 5 min.

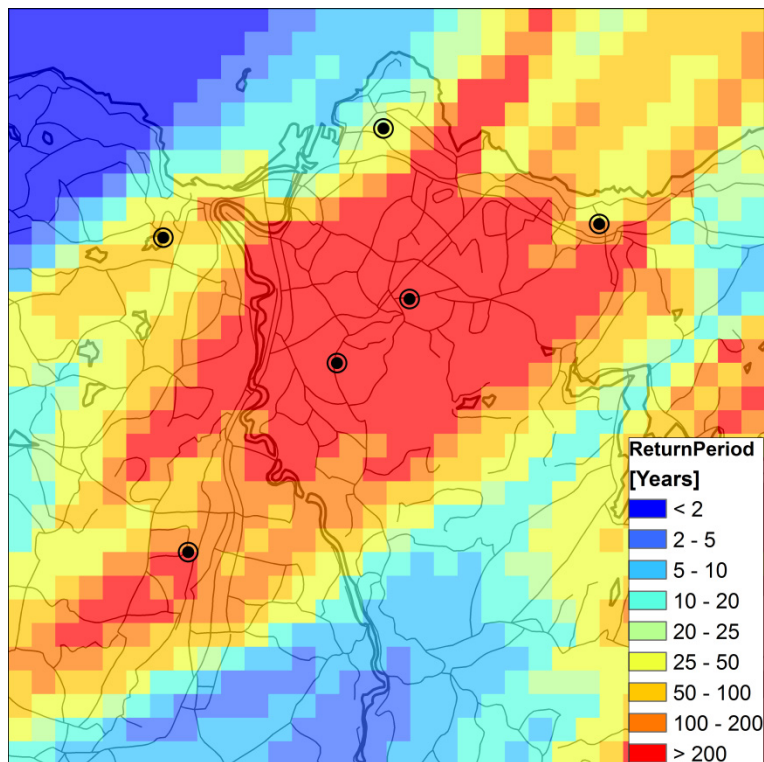


**Figure 16.** Longest return periods for the event on August 13 2007. The return period for each pixel corresponds to the longest period out of the return periods estimated for the maximum intensities for the following durations: 1, 5, 15, 15 and 20 min.

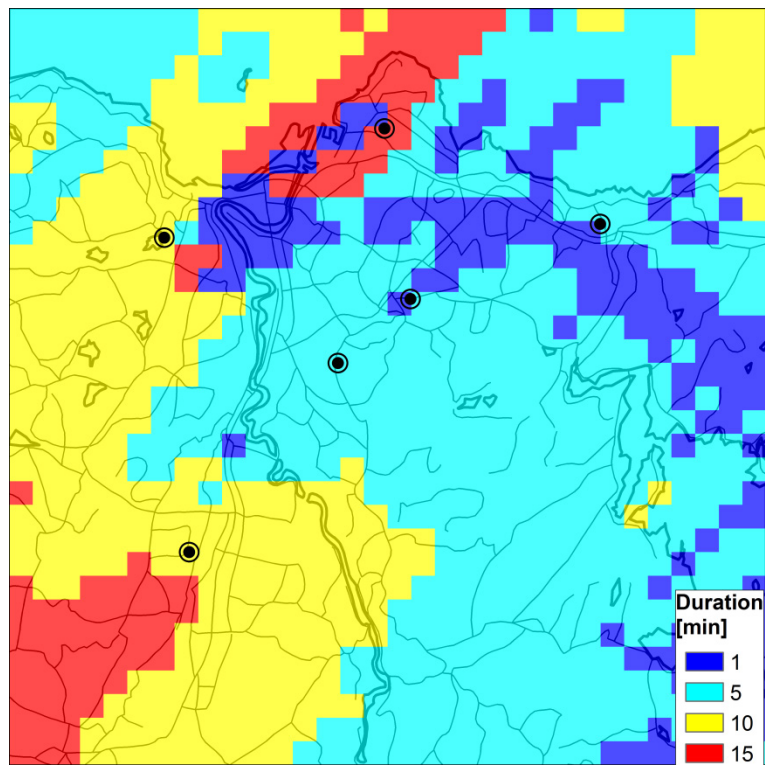


Figure 17. Durations corresponding to the longest return periods shown in the map of Figure 16.

## 5 Summary and conclusions

A tool has been developed in this project for automatically estimating spatially distributed return periods using radar measurements. The following processing steps have been implemented in the tool for achieving this estimation:

- Correction for signal attenuation
- Projection and conversion from polar to cartesian coordinates
- Z-R conversion
- Temporal interpolation using advection
- Adjustment using rain gauge measurements
- Temporal accumulation
- Return period estimation

The tool was applied on two extreme rainfall events in Trondheim which occurred on July 29 2007 and August 13 2007. The following conclusion can be drawn from these applications:

- The tool enables a fully-automated estimation of return periods using readily available data.
- The advection-based interpolation helps capture the temporal variation in rainfall intensity.
- After adjustment using gauge measurements, the Rissa radar measurements can be used to estimate quantitatively reasonable rainfall accumulations over Trondheim.
- Accumulated rainfall maps generated from distributed radar measurements give spatial distributions which are completely different from distribution generated from gauge-interpolated maps. Maps interpolated from point gauge measurements have less information about the spatial distribution of precipitation since they depend on the location and density of gauges.
- The network of six gauges in Trondheim can miss the areas with the maximum rainfall intensities during the passage of convective events over the city.

## 6 Further research

The following issues need further research and can potentially lead to improved results if pursued.

- The parameters for the attenuation correction were obtained from literature (Hazenberget al. 2011) and may be unrepresentative for the region and for the type of events analysed. Applying parameters derived from drop size distribution measurements for similar type of events in the same region may reduce the uncertainties associated with the attenuation correction.
- To account for the errors related to the uncertainties in the parameters of the Z-R relation, MFB adjustment has been applied. Such an adjustment does not consider the spatial variability of these parameters. However, it has been previously documented that Z-R relations can vary both from storm-to-storm and within the same storm (Uijlenhoet et al. 2003; Ulbrich and Lee 1999). A method accounting for this variability and thereby enabling a spatially variable correction may lead to improved quantitative accuracy.
- The advection vector estimation was carried out using logarithmic reflectivity ( $10 \cdot \log Z$ ). If the estimation is applied to linear rain rate or linear reflectivity, the locations with heavy rain will dominate the result. This means that the matching reduces to a few pixels of high intensity. The use of logarithmic scale significantly reduces this influence. It should, however, be investigated if this is a desirable effect in the context of extreme convective rainfall analyses.
- The temporal interpolation of radar rainfall rates assumes linear variation in rates. The validity of this assumption can be assessed and possibly other forms of variation identified as being more accurate.
- In this report return periods were estimated for pixels. It would be interesting to estimate the return period for catchment rainfall as well. This would require an estimate of area reduction factors for extreme precipitation as well as a map of drainage directions that might allow estimating return periods in every point along a drain or stream.

## 7 References

- Abdella, Y. and K. Alfredsen (2010), Long-term evaluation of gauge-adjusted precipitation estimates from a radar in Norway, *Hydrology Research*, 41, 171-192.
- Delrieu, G., L. Huc, and J. D. Creutin (1999), Attenuation in rain for X and C-band weather radar systems: Sensitivity with respect to the drop size distribution, *J. Appl. Meteorol.*, 38, 57–68.
- Delrieu, G., H. Andrieu and J. D. Creutin (2000), Quantification of path-integrated attenuation for X- and C-Band weather radar systems operating in Mediterranean heavy rainfall, *J. Appl. Meteorol.*, 39, 840– 850.
- Doviak, R. J., and D. S. Zrnić (1993), *Doppler Radar and Weather Observations*, 2nd ed, Academic Press.
- Fabry, F., A. Bellon, M. R. Duncan and G. L. Austin (1994), High resolution rainfall measurements by radar for very small basins: the sampling problem reexamined, *J. Hydrol.*, 161, 415-428.
- Hannesen, R., and H. Gysi (2002), An enhanced precipitation accumulation algorithm for radar data, in *Proceedings of the Second European Conference on radar Meteorology (ERAD)*, pp. 266-271, Delft, Netherlands.
- Hazenberg, P., H. Leijnse and R. Uijlenhoet (2011), Radar rainfall estimation of stratiform winter precipitation in the Belgian Ardennes, *Water Resour. Res.*, 47, W02507, doi:10.1029/2010WR009068.
- Li, L., W. Schmid, and J. Joss (1995), Nowcasting of motion and growth of precipitation with radar over a complex orography, *J. Appl. Meteorol.*, 34, 1286–1300.
- Liu, C. and W.F. Krajewski (1996), A comparison of methods for calculation of radar-rainfall hourly accumulations, *Water Resources Bulletin*, 32(2), 305-315.
- Marshall, J. S., and W. M. K. Palmer (1948), The distribution of raindrops with size, *J. Meteorol.*, 5, 165–166.
- Piccolo, F., and G. B. Chirico (2005), Sampling errors in rainfall measurements by weather radar, *Advances in Geosciences*, 2, 151-155.
- Risholt, L. P. (2009), Kjelleroversvømmelser i Trondheim sommeren 2007, Rapport nr 571451-1, Sweco.
- Steiner, M., J.A. Smith, S.J. Burges, C.V. Alonso, and R.W. Darden (1999), Effect of bias adjustment and rain gauge data quality control on radar rainfall estimation, *Water Resour. Res.*, 35(8), 2487-2503.
- Thorolfsson, S. T., L. P. Risholt, O. Nilsen, A. Ellingsson, V. Kristiansen, Ø. Hagen and E. Karlsen (2008), Extreme rainfalls and damages on August 13 2007 in the city of Trondheim, Norway, in *Northern Hydrology and its global role: XXV Nordic Hydrological Conference*, pp. 295-301, Nordic Hydrological Programme, Reykjavík, Iceland.
- Uijlenhoet, R., and A. Berne (2008), Stochastic simulation experiment to assess radar rainfall retrieval uncertainties associated with attenuation and its correction, *Hydrol. Earth Syst. Sci.*, 12, 587– 601, doi:10.5194/hess-12-587-2008.

Uijlenhoet, R., M. Steiner and J.A. Smith (2003), Variability of raindrop size distributions in a squall line and implications for radar rainfall estimation, *J. Hydrometeorol.*, 4(1), 43–61.

Ulbrich, C.W., and L.G. Lee (1999), Rainfall measurement error by WSR-88D radars due to variations in the Z-R law parameters and the radar constant, *J. Atmos. Oceanic Technol.*, 16, 1017 – 1024.

Villarini, G., and W. F. Krajweski (2010), Review of the different sources of uncertainty in single polarization radar-based estimates of rainfall, *Surveys in Geophysics*, 31, 107-129.



Technology for a better society

[www.sintef.no](http://www.sintef.no)